J. Fluid Mech. (1974), *vol.* **64**, *part* 4, *pp.* 763–774
Printed in Great Britain

Evolution of a moderately short turbulent boundary layer in a severe pressure gradient

By R. G. DEISSLER

Lewis Research Center, National Aeronautics and Space Administration,
Cleveland, Ohio 44135

(Received 20 July 1973)

The early and intermediate development of a highly accelerated (or decelerated) turbulent boundary layer is analysed. For sufficiently large accelerations (or pressure gradients) and for total normal strains which are not excessive, the equation for the Reynolds shear stress simplifies to give a stress that remains approximately constant as it is convected along streamlines. The theoretical results for the evolution of the mean velocity in favourable and adverse pressure gradients agree well with experiment for the cases considered. A calculation which includes mass injection at the wall is also given.

1. Introduction

Although the general problem of turbulent shear flow is extremely complex, solutions can be obtained for certain simplified cases. Most of the cases in which analytical progress has been made are initial-value problems rather than fully developed flows, the latter apparently requiring the consideration of high-order effects. For instance, essentially complete solutions can be obtained for the effect of uniform mean gradients on developing locally homogeneous turbulence without self-interaction (e.g. Pearson 1959; Deissler 1961, 1968, 1971, 1972). Much of the information obtained from the simplified models is applicable to more complicated cases.

Another initial-value problem which can evidently be analysed is that of the evolution, from a given initial state, of a moderately short, highly accelerated turbulent boundary layer. For that problem a simplification of the equations of motion allows us to consider the Reynolds shear stress to be approximately constant along streamlines. The simplification is applicable when the total longitudinal strain is not excessive and a pressure-gradient parameter is sufficiently large. Thus, although the present problem might seem at first to be more complicated than say the fully developed problem, it turns out to be relatively tractable within the framework of the present simplification.

The simplification of frozen Reynolds stress will be considered in detail in the analysis section. It will suffice for now to treat the present case as the opposite of the equilibrium boundary layer. In the latter boundary layer changes are so gradual that the turbulence is in quasi-equilibrium with local conditions at each point, and initial conditions are of little importance. The experiments of

Blackwelder & Kovasznay (1972) suggest the validity of the simplification used here for severe gradients, since although the pressure gradients caused the mean flow in those experiments to change considerably, the Reynolds stresses, at least in the important intermediate region of wall distances, were relatively unaffected. The region considered in the present analysis is mainly the so-called relaminarization region for severe favourable pressure gradients which has been observed, for instance, in experiments of Kline *et al.* (1967), Patel & Head (1968) and Blackwelder & Kovasznay (1972). A few results are also given for mass injection at the wall and for severe adverse pressure gradients.

2. Analysis

The equation for the mean velocity in an incompressible turbulent flow is

$$\frac{\partial U_i}{\partial t}+U_k\frac{\partial U_i}{\partial x_k}=-\frac{1}{\rho}\frac{\partial P}{\partial x_i}+\frac{\partial}{\partial x_k}\left(\nu\frac{\partial U_i}{\partial x_k}-\overline{u_iu_k}\right), \tag{1}$$

where U_i is a mean velocity component, u_i is a turbulent velocity component, x_i is a space co-ordinate, t is the time, ρ is the density, ν is the kinematic viscosity and P is the mean pressure. The overbar designates an averaged quantity, and the summation convention is used. For a thin steady-state two-dimensional boundary layer, (1) becomes

$$U_1\frac{\partial U_1}{\partial x_1}=-U_2\frac{\partial U_1}{\partial x_2}-\frac{1}{\rho}\frac{dP}{dx_1}+\nu\frac{\partial^2U_1}{\partial x_2^2}-\frac{\partial}{\partial x_2}\overline{u_1u_2}, \tag{2}$$

where x_1 is in the direction of the main flow and P is a function only of x_1. The transverse velocity U_2 is given by the continuity relation for the mean flow

$$\partial U_2/\partial x_2=-\partial U_1/\partial x_1 \tag{3}$$

and dP/dx_1 is specified as a function of x_1.

Equations (2) and (3) can be written in dimensionless form as

$$\frac{1}{2}\frac{\partial U_1^{*2}}{\partial x_1^*}=-U_2^*\frac{\partial U_1^*}{\partial x_2^*}-\frac{\nu}{\rho U_0^3}\frac{dP}{dx_1}+\frac{\partial^2U_1^*}{\partial x_2^{*2}}-\frac{\partial(\overline{u_1u_2})^*}{\partial x_2^*} \tag{4}$$

and

$$\partial U_2^*/\partial x_2^*=-\partial U_1^*/\partial x_1^*, \tag{5}$$

where

$$U_i^*=U_i/U_0,\quad x_i^*=x_iU_0/\nu,\quad (\overline{u_iu_j})^*=\overline{u_iu_j}/U_0^2$$

and U_0 is a constant reference velocity, say the velocity outside the boundary layer at the initial station.

In order to solve (4) and (5) to obtain the evolution of U_1^*, the Reynolds shear stress $\overline{u_1u_2}$ must be known at each point in the flow. The full two-point equations for the turbulent stresses have been given (Deissler 1961, equations (5), (7) and (8)), and can be written in abbreviated dimensionless form for the steady-state case as

$$\begin{aligned}\tfrac{1}{2}(U_1'^*+U_1''^*)\frac{\partial(\overline{u_i'u_j''})^*}{\partial x_1^*}&=-\tfrac{1}{2}(U_2'^*+U_2''^*)\frac{\partial(\overline{u_i'u_j''})^*}{\partial x_2^*}-(\overline{u_k'u_j''})^*\frac{\partial U_i'^*}{\partial x_k'^*}+\dots\\&-\frac{1}{2}\frac{\partial(\overline{u_i'u_j''u_k''})^*}{\partial x_k^*}+\dots+\frac{\partial(\overline{p'u_j''})^*}{\partial r_i^*}-\frac{\partial(\overline{u_i'p''})^*}{\partial r_j^*}+\dots+\frac{1}{2}\frac{\partial^2(\overline{u_i'u_j''})^*}{\partial x_k^*\,\partial x_k^*}+2\frac{\partial^2(\overline{u_i'u_j''})^*}{\partial r_k^*\,\partial r_k^*},\end{aligned} \tag{6}$$

$$\frac{1}{4}\frac{\partial^2(\overline{u_i' p''})^*}{\partial x_j^* \partial x_j^*} + \ldots = -2\frac{\partial U_j''^*}{\partial x_k''^*}\left(\frac{1}{2}\frac{\partial(\overline{u_i' u_k''})^*}{\partial x_j^*} + \frac{\partial(\overline{u_i' u_k''})^*}{\partial r_j^*}\right) - \frac{1}{4}\frac{\partial^2(\overline{u_i' u_j'' u_k''})^*}{\partial x_j^* \partial x_k^*} + \ldots, \quad (7)$$

with a similar equation for $(\overline{p' u_j''})^*$, where, as in (4) and (5), the starred quantities have been non-dimensionalized by suitable combinations of U_0, ν and ρ, and p is the fluctuating pressure component. The primes and double primes designate quantities evaluated at points P' and P'', which are separated by the vector $\mathbf{r}$, and the unprimed quantities are measured at x_i, which lies halfway between P' and P''.

Equations (6) and (7) contain triple velocity correlations which can be obtained from three-point equations. The latter contain quadruple correlations which in turn can be obtained from four-point equations, and so on. Thus an infinite hierarchy of equations results. Equation (6), for $r_i = 0$, becomes

$$U_1^* \frac{\partial(\overline{u_i u_j})^*}{\partial x_1^*} = -U_2^* \frac{\partial(\overline{u_i u_j})^*}{\partial x_2^*} - (\overline{u_2^2})^* \frac{\partial U_1^*}{\partial x_2^*} - \frac{\partial(\overline{u_1 u_2^2})^*}{\partial x_2^*} + \ldots. \quad (8)$$

Each of the infinite hierarchy of higher-order equations can be put into a dimensionless form similar to that of (4)–(8). Thus, for a given initial flow field the flow field at any position along the boundary layer is given by the functional equations

$$\frac{U_1}{U_0} = f_1\left(\frac{x_1 U_0}{\nu}, \frac{x_2 U_0}{\nu}, \frac{\nu}{\rho U_0^3}\frac{dP}{dx_1}\right), \quad (9)$$

$$\frac{\overline{u_i u_j}}{U_0^2} = f_2\left(\frac{x_1 U_0}{\nu}, \frac{x_2 U_0}{\nu}, \frac{\nu}{\rho U_0^3}\frac{dP}{dx_1}\right) \quad (10)$$

and an infinite hierarchy of similar equations for other turbulence quantities. Specification of the parameters on the right side of (9) or (10) will therefore, in principle, allow the determination of the mean flow and turbulence fields.

New parameters obtained by operating on the parameters in (9) or (10) can, of course, be used in their place, so long as the same total number is maintained. Thus, one of the original parameters can be replaced by U_∞/U_0, where U_∞ is the velocity at the edge of the boundary layer, since

$$-\frac{1}{\rho}\frac{dP}{dx_1} = U_\infty \frac{dU_\infty}{dx_1} \quad (11)$$

and

$$-\int_0^{x_1^*} \frac{\nu}{\rho U_0^3}\frac{dP}{dx_1} dx_1^* = \int_0^{x_1^*} \frac{\nu U_\infty}{U_0^3}\frac{dU_\infty}{dx_1} dx_1^*$$

$$= \int_{U_0}^{U_\infty} \frac{U_\infty dU_\infty}{U_0^2} = \frac{1}{2}\left(\frac{U_\infty}{U_0}\right)^2 - \tfrac{1}{2}. \quad (12)$$

Equations (4) and (8) can be transformed from (x_1, x_2) to (x_1, ψ) co-ordinates (von Mises co-ordinates), where the stream function ψ is given by

$$\partial\psi/\partial x_1 = -U_2, \quad \partial\psi/\partial x_2 = U_1. \quad (13)$$

The result for $i = 1, j = 2$ is

$$\frac{1}{2}\left(\frac{\partial U_1^{*2}}{\partial x_1^*}\right)_\psi = -\frac{\nu}{\rho U_0^3}\frac{dP}{dx_1} + \tfrac{1}{2}U_1^* \frac{\partial^2 U_1^{*2}}{\partial\psi^{*2}} - U_1^* \frac{\partial(\overline{u_1 u_2})^*}{\partial\psi^*} \quad (14)$$

and

$$\left(\frac{\partial(\overline{u_1 u_2})^*}{\partial x_1^*}\right)_\psi = -(\overline{u_2^2})^* \frac{\partial U_1^*}{\partial\psi^*} - \frac{\partial(\overline{u_1 u_2^2})^*}{\partial\psi^*} + \ldots \equiv R_{12}, \quad (15)$$

where the continuity equation (5) and the boundary-layer assumptions have been used to simplify the production term in (15) (first term on the right side), and $\psi^* = \psi/\nu$. Equation (15) can be integrated along a streamline to give

$$(\overline{u_1 u_2})^* = (\overline{u_1 u_2})_0^* + \int_1^{U_1^0} \frac{R_{12}(dU_1^0)_\psi}{[\nu/U_0 U_{10}](\partial U_1/\partial x_1)_\psi}, \tag{16}$$

where $U_1^0 = U_1/U_{10}$. The quantities U_{10} and $(\overline{u_1 u_2})_0^*$ are, respectively, the values of U_1 and $(\overline{u_1 u_2})^*$ on the same streamline as U_1 and $(\overline{u_1 u_2})^*$ but at the initial station, and U_0 is the value of U_∞ at the initial station. The subscript ψ indicates changes along a streamline. We assume that R_{12} is not a strong function of $\partial U_1/\partial x_1$, since R_{12} does not contain $\partial U_1/\partial x_1$ explicitly [equation (15)]. Also R_{12} will, at least initially, be close to zero, since for the initial zero-pressure-gradient boundary layer, the shear production term is in approximate equilibrium with the other terms in R_{12}. Then for sufficiently large $[\nu/U_0 U_{10}](\partial U_1/\partial x_1)_\psi$ (or large $(-\nu/\rho U_0^3)\, dP/dx_1$), and/or for U_1/U_{10} (or U_∞/U_0) sufficiently close to one, (16) reduces to

$$\overline{u_1 u_2} \approx \overline{u_1 u_2}(\psi) = [\overline{u_1 u_2}(\psi)]_0. \tag{17}$$

That is, if the pressure-gradient parameter (or the acceleration along streamlines) is sufficiently large and the total normal strain $\ln(U_\infty/U_0)$ is not excessive, the Reynolds shear stress can be considered as frozen at its initial values as it is convected along streamlines. In that case $\overline{u_1 u_2}$ for a particular flow is, of course, a function only of ψ. Equation (17) can be written alternatively as

$$U_1(\partial \overline{u_1 u_2}/\partial x_1)_\psi = U_k\, \partial \overline{u_1 u_2}/\partial x_k = 0. \tag{17a}$$

Equation (16) indicates that the allowable values of the parameters are interdependent. For instance for U_1/U_{10} (or U_∞/U_0) quite close to one, (17) may apply reasonably well even when the pressure gradient (or $\partial U_1/\partial x_1$) is moderately small. Conversely, for very large pressure gradients (or large $\partial U_1/\partial x_1$) it may be allowable to have relatively large departures of U_1/U_{10} (or of U_∞/U_0) from one.

In order to get an idea of how important an effect normal strains might have on $\overline{u_1 u_2}$, it may be instructive to consider analytical results for locally homogeneous turbulence with uniform normal strain and shear without turbulence self-interaction (Deissler 1968, 1972). The results for $\overline{u_1 u_2}$ for $(\partial U_1/\partial x_2)/(\partial U_1/\partial x_1) = 2$ are given in figure 1. The point where $U_1 = U_{10}$ is taken where $\partial \overline{u_1 u_2}/\partial x_1$ is close to zero, since that corresponds to the zero-pressure-gradient region of a boundary layer upstream of a pressure-gradient region. For values of $U_1/U_{10} \leqslant 2$, $\overline{u_1 u_2}$ according to figure 1 should not vary by more than about 14%. For larger values of U_1/U_{10} the variation of $\overline{u_1 u_2}$ is somewhat greater. However, the variation of $\overline{u_1 u_2}$ in an actual boundary layer, where the turbulence is inhomogeneous and the parameter $(\partial U_1/\partial x_2)/(\partial U_1/\partial x_1)$ is usually much greater than 2, appears to be less than that indicated in figure 1 (see results of Blackwelder & Kovasznay).

3. Results and discussion

Equations (14) and (17) have been integrated numerically along streamlines to determine the evolution of several boundary layers in severe pressure gradients. The numerical integrations were carried out by using an implicit method which

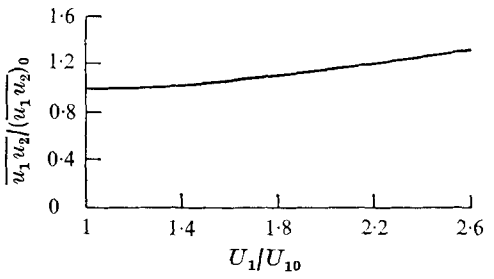

FIGURE 1. Theoretical results for development of $\overline{u_1u_2}$ in homogeneous turbulence with uniform velocity gradients and no turbulence self-interaction (Deissler 1968, 1972, with $(\partial U_1/\partial x_2)/(\partial U_1/\partial x_1) = 2$).

was stable for all ratios of longitudinal to transverse increments. Because of the steep gradients close to the wall, more points were used in that region. The boundary conditions used for (14) were $U_1 = 0$ at the wall and $U_1 = U_\infty$ at the edge of the boundary layer. Since U_1/U_∞ varies more slowly with x_1 than does U_1 itself, the former was used as the dependent variable in the calculations. Initial values of U_1 and $\overline{u_1u_2}$ and longitudinal pressure distributions for the data of Patel & Head (1968) and of Blackwelder & Kovasznay (1972) were used in the calculations for favourable pressure gradients, and the predicted results were compared with data from those experiments. Neither of those sets of data gave initial values of $\overline{u_1u_2}$ close to the wall, so for that region the relation

$$(\overline{u_1u_2})_0 = \nu(\partial U_1/\partial x_2)_0 - \tau_{w0}/\rho \tag{18}$$

was used, since close to the wall for small pressure gradients the total shear stress does not vary appreciably from the value τ_w at the wall. The subscripts 0 refer to values at the initial station. Patel & Head also did not give values of $\overline{u_1u_2}$ for the region away from the wall, so for that range of their wall distances $[(\tau_{w0}/\rho)^{\frac{1}{2}}x_2/\nu > 45]$ $\overline{u_1u_2}$ was obtained from Hinze's (1959) plot of Klebanoff's zero-pressure-gradient data. Patel & Head's data for the thinner boundary layer (22 in. entry) were used, since those correspond closely to two-dimensional conditions. Initial conditions were specified at 936 cm in Blackwelder & Kovasznay's experiment and at -5 in. in that of Patel & Head.

Velocity profiles (U_1/U_∞ against ψ/ν) are plotted and compared with experiment in figures 2(*a*) and (*b*). (Note the shifted vertical scales.) In all cases the effect of the pressure gradient and the total normal strain parameter U_∞/U_0 is to flatten the profiles. The agreement between theory and experiment is considered good.

Semi-logarithmic plots of $U_1/(\tau_w/\rho)^{\frac{1}{2}}$ against $(\tau_w/\rho)^{\frac{1}{2}}x_2/\nu$ (law-of-the-wall plots) are given in figure 3. These profiles show the inner region of the boundary layer much better than do figures 2(*a*) and (*b*). The shear stress τ_w at the wall for the theoretical curves was obtained from the slope of the velocity profile at the wall by using points very close to the wall ($(\tau_w/\rho)^{\frac{1}{2}}x_2/\nu \ll 1$). Points very close to the wall were necessary because of the nonlinearity of the profile close to the wall in the presence of a pressure gradient. It might be pointed out that this nonlinearity makes the experimental determination of the shear stress at the wall extremely difficult. Both theory and experiment indicate that the original

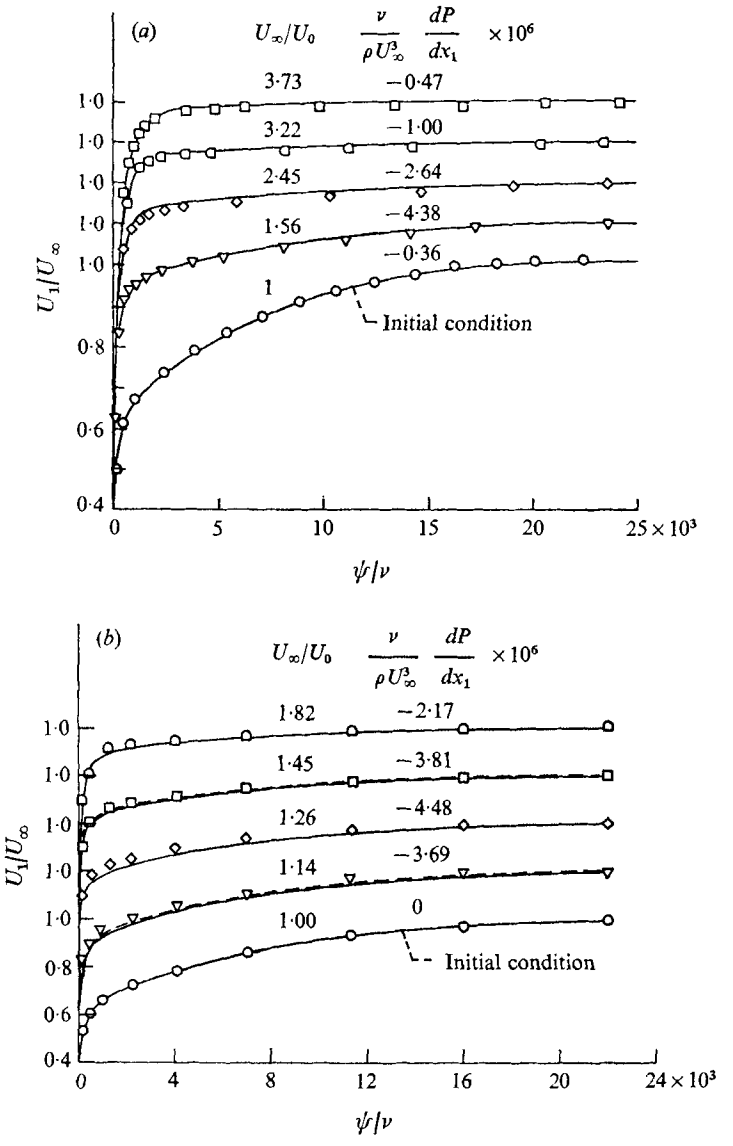

FIGURE 2. Predicted early and intermediate development of mean velocity profile in a turbulent boundary layer with severe favourable pressure gradients and comparison with experiments of (*a*) Blackwelder & Kovasznay (1972) and (*b*) Patel & Head (1968). (Note shifted vertical scales.) ——, theory, equations (17) and (14); – – –, $\overline{u_1 u_2} = 0$; points, experiment.

logarithmic and wake regions are destroyed by the pressure-gradient and normal-strain effects, although a new logarithmic layer of smaller slope seems to form eventually. Also the thickness of the sublayer approximately doubles, indicating an apparent 'relaminarization', as observed experimentally by many investigators. However, it is not a true relaminarization since, at least in the theory, $\overline{u_1 u_2}$ is constant along streamlines. The agreement between theory and

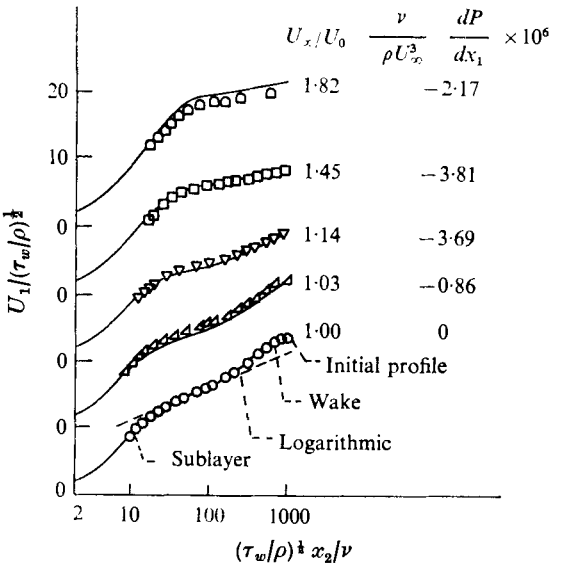

FIGURE 3. Semi-logarithmic law-of-the-wall plot of theoretical velocity profiles for severe favourable pressure gradients and comparison with experiment of Patel & Head (1968). (Note shifted vertical scales.) ——, theory, equations (17) and (14); points, experiment.

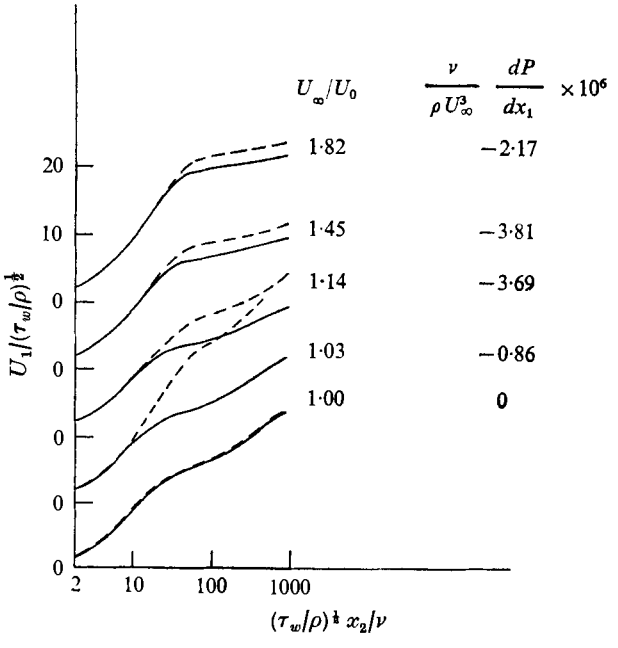

FIGURE 4. Effect of neglecting Reynolds shear stress on theoretical law-of-the-wall plot for experimental conditions of figure 3. (Note shifted vertical scales.) ——, theory, equations (17) and (14); – – –, $\overline{u_1 u_2} = 0$.

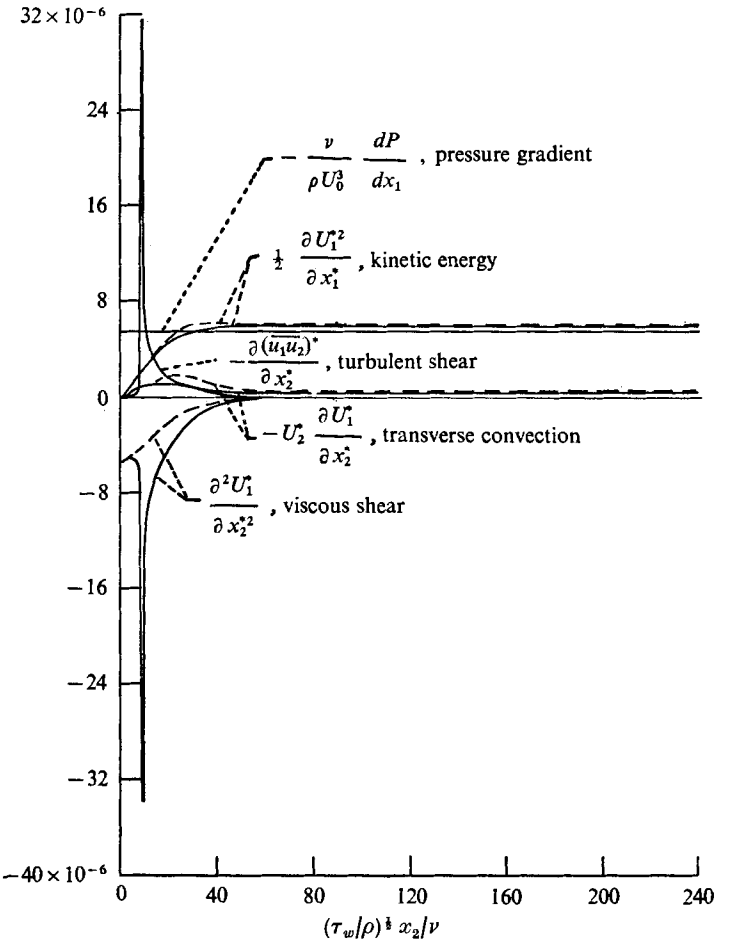

FIGURE 5. Contribution of various terms in (4) to rate of change of dimensionless kinetic energy of mean flow for conditions of figure 3. $U_\infty/U_0 = 1{\cdot}14$. ——, theory, equations (17) and (14); – – –, $\overline{u_1u_2} = 0$.

experiment appears to be quite good. For values of U_∞/U_0 larger than those shown, the approximation of a frozen Reynolds stress apparently begins to break down.

In order to see how sensitive the development of the mean profile is to the Reynolds shear stress, results were calculated for $\overline{u_1u_2} = 0$ and are shown dashed in figures 2(*b*) and 4. The effect of $\overline{u_1u_2}$ on the profiles in figure 2(*b*) is slight. The law-of-the-wall plots in figure 4, on the other hand, show a significant quantitative effect of $\overline{u_1u_2}$ on the profiles, but qualitatively the curves for $\overline{u_1u_2} = 0$ and $\overline{u_1u_2} \neq 0$ are much the same. In both cases the original logarithmic and wake regions are destroyed and the sublayer is thickened. The difference between the indicated quantitative effects of $\overline{u_1u_2}$ on the profiles in figures 2(*b*) and 4 is evidently due to the difference in scales and in scaling parameters in the two figures.

Figure 5 shows, for a large value of the pressure-gradient parameter, the contributions of various terms in (4) to the rate of change of the non-dimensional

mean kinetic energy $\frac{1}{2}\partial(U_1/U_0)^2/\partial(x_1 U_0/\nu)$. (The energy in the transverse velocity component is negligible for a boundary layer.) The contribution of the Reynolds stress term is very large in a narrow region near the wall. However, that tends to be offset by the viscous contribution, as might be expected from (18). Comparison of the curves for $\overline{u_1 u_2} = 0$ and $\overline{u_1 u_2} \neq 0$ shows that the viscous contribution adjusts its value so as to offset the effect of the Reynolds stress. (At the initial station, (18) indicates that the two terms should exactly balance.) The viscous term is not zero at the wall but balances the pressure-gradient term so that U_1 can remain zero at the wall. Thus, the present velocity profile, in contrast to the case of zero pressure gradient, is nonlinear at the wall. (If it were linear the viscous term in (4) would be zero at the wall.)

The pressure-gradient term is independent of wall distance and, for the case shown in figure 5, becomes dominant for $(\tau_w/\rho)^{\frac{1}{2}} x_2/\nu > 40$. Thus, the destruction of the logarithmic and wake regions is due mainly to the pressure-gradient term, rather than to a change in the structure of the turbulence (although some change in structure may occur (Kline *et al.* 1967)). Also, the thickening of the sublayer is mostly, although not entirely, due to the pressure-gradient contribution, since as mentioned, viscous effects tend to offset the Reynolds stress contribution.

The results in figure 5 are, of course, for a large pressure-gradient parameter. For regions of lower pressure gradient, the Reynolds stress will have a greater effect, as shown in figure 4. Also, the velocity profile at any position depends on the whole distribution of pressure gradients up to that position; that is, U_1 is a functional of dP/dx_1, or

$$U_1 = U_1[dP(\xi)/dx_1],$$

where $0 < \xi < x_1$. Thus, there is a quantitative (but not a qualitative) effect of $\overline{u_1 u_2}$ on the velocity profile, even at those positions where the pressure-gradient parameter is large.

The analysis can be easily extended to include mass injection at the wall by transforming (14) from (x_1, ψ) to (x_1, ψ') co-ordinates, where $\psi' = \psi - \psi_w$, and ψ_w is the stream function at the wall. The latter will vary with x_1 in accordance with (13). Equation (14), when written in (x_1, ψ') co-ordinates, has the additional term $-\frac{1}{2}[U_{2w}/U_0]\,\partial U_1^{*2}/\partial\psi'^*$ on the right side, where U_{2w} is the normal velocity at the wall. As before we use the simplification that $\overline{u_1 u_2}$ remains frozen as it is convected along streamlines (along lines of constant ψ, not constant ψ'). The injected fluid is assumed to be turbulence-free.

To show the effect of mass injection on a boundary layer with severe pressure gradients, mass injection was added in the theoretical calculations in figure 3. For positive mass injection figure 6 shows that the normal flow quickly raises the $U_1/(\tau_w/\rho)^{\frac{1}{2}}$ curve, particularly in the wake region, after which the favourable pressure gradient lowers and flattens the curve. The resulting curve still lies above the initial profile. For negative injection, the normal flow and pressure gradient lower and flatten the initial profile. These trends are similar to those observed by Julien, Kays & Moffat (1971).

All of the results so far were for favourable pressure gradients, but the analysis should apply as well to severe unfavourable gradients. Figure 7 shows a comparison between theory and experiment for the results of Kline *et al.* for a

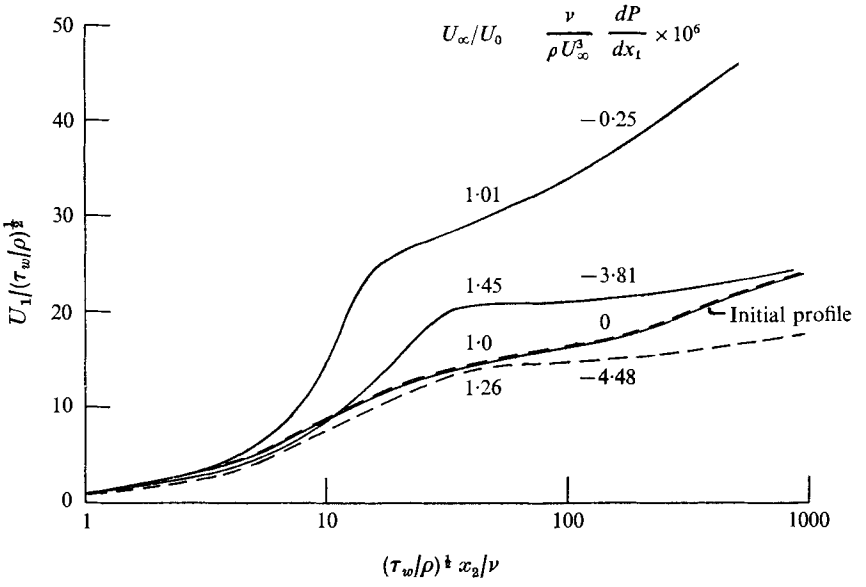

FIGURE 6. Effect of mass injection normal to wall on theoretical velocity profiles for severe favourable pressure gradients. (Initial conditions and pressure gradients correspond to figure 3.) ——, $U_{2w}/U_0 = 0{\cdot}002$; – – –, $U_{2w}/U_0 = -0{\cdot}002$.

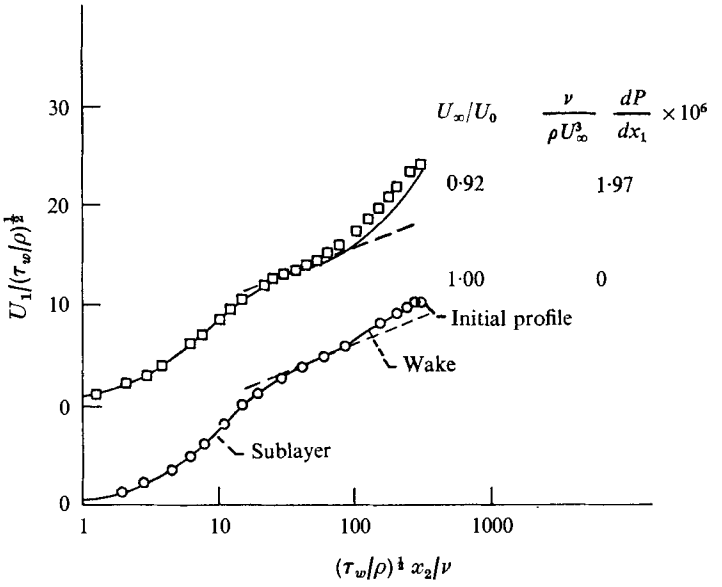

FIGURE 7. Theoretical velocity profiles for severe adverse pressure gradients and comparison with experiment of Kline *et al.* (1967). (Note shifted vertical scales.) ——, theory, equations (17) and (14); – – –, logarithmic; ○, □, experiment.

severe unfavourable pressure gradient (their figure 9*a*). The results indicate that the adverse pressure gradients produce an exaggerated wake region, but that the logarithmic and sublayer regions are relatively unaffected. The agreement between theory and experiment is good. It might be mentioned that the results for adverse pressure gradients were more sensitive to the $\overline{u_1 u_2}$ distribution than were those for favourable gradients. In particular, when $\overline{u_1 u_2}$ was taken as zero, separation occurred upstream for the run shown in figure 7 for $U_\infty/U_0 = 0{\cdot}92$. Thus the presence of turbulence appears to delay separation. This is evidently because the Reynolds stress term in (4) is positive close to the wall and thus tends to increase U_1 in that region.

4. Concluding remarks

The use of a Reynolds shear stress which remains frozen at its initial values as it is convected along streamlines in a moderately short, highly accelerated boundary layer gives results in agreement with experiment for favourable and unfavourable pressure gradients. For favourable pressure gradients both theory and experiment showed a flattening of the mean velocity profile with destruction of the original logarithmic and wake regions, and a thickening of the sublayer region. Those effects occurred both when the Reynolds shear stress was uniform along streamlines and when it was zero, although there were significant quantitative differences between the profiles in the two cases. Thus at least for the favourable-pressure-gradient cases considered here, the Reynolds stress term in the equation for the evolution of the mean velocity profile appears to be somewhat less important than the pressure-gradient term. Positive mass injection normal to the wall decreased the shear stress at the wall, whereas negative injection had the opposite effect.

The effect of adverse pressure gradients on the wake region of the velocity profile was opposite to that of the favourable gradients; that is, the unfavourable gradients produced an exaggerated wake region. However, the logarithmic and sublayer regions were relatively unaffected for the case calculated. In contrast to the favourable-pressure-gradient case, the presence of turbulence affected the adverse-gradient results both quantitatively and qualitatively. In particular, turbulence prevented the early development of a separation profile, apparently because the Reynolds stress term in (4) is positive close to the wall.

The simplification of constant Reynolds shear stress along streamlines was found most applicable when a pressure-gradient parameter was reasonably large and the total normal strain was not excessive [equation (16)].

Because of the practical importance of heat transfer in highly accelerated flows, heat transfer coefficients corresponding to experimental situations have been calculated using the present method (Deissler 1974). Those results show agreement between theory and experiment for the conditions indicated in the preceding paragraph.

REFERENCES

BLACKWELDER, R. F. & KOVASZNAY, L. S. G. 1972 *J. Fluid Mech.* **53**, 61.

DEISSLER, R. G. 1961 *Phys. Fluids*, **4**, 1187.

DEISSLER, R. G. 1968 *J. Math. Phys.* **47**, 310.

DEISSLER, R. G. 1971 *Z. angew. Math. Phys.* **22**, 267.

DEISSLER, R. G. 1972 *Phys. Fluids*, **15**, 1918.

DEISSLER, R. G. 1974 *Int. J. Heat Mass Transfer* (to be published).

HINZE, J. O. 1959 *Turbulence*, p. 491. McGraw-Hill.

JULIEN, H. L., KAYS, W. M. & MOFFAT, R. J. 1971 *J. Heat Transfer*, **93**, 373.

KLINE, S. J., REYNOLDS, W. C., SCHRAUB, F. A. & RUNSTADLER, P. W. 1967 *J. Fluid Mech.* **30**, 741.

PATEL, V. C. & HEAD, M. R. 1968 *J. Fluid Mech.* **34**, 371.

PEARSON, J. R. A. 1959 *J. Fluid Mech.* **5**, 274.